Journal of Steroid Biochemistry & Molecular Biology 116 (2009) 86–92

Contents lists available at ScienceDirect

Journal of Steroid Biochemistry and Molecular Biology

journal homepage: www.elsevier.com/locate/jsbmb

Osteoblastogenic effects of dexamethasone through upregulation of TAZ expression in rat mesenchymal stem cells

Dun Hong[a,b], Hai-Xiao Chen[b,*], Yun Xue[a], Dong-Mei Li[a], Xiao-Chen Wan[a], Renshan Ge[c], Ji-Cheng Li[a,**]

[a] Institute of Cell Biology, Medical College of Zhejiang University, 388 Yuhangtang Road, Hangzhou 310058, Zhejiang Province, China
[b] Orthopedic Department, Taizhou Hospital, Wenzhou Medical College, Linhai 317000, Zhejiang Province, China
[c] Population Council, 1230 York Avenue, New York, NY 10021, USA

ARTICLE INFO

Article history:
Received 22 November 2008
Received in revised form 4 May 2009
Accepted 8 May 2009

Keywords:
Dexamethasone
TAZ
Mesenchymal stem cells
Osteoblastic differentiation

ABSTRACT

Transcriptional coactivator with PDZ-binding motif (TAZ), a β-catenin-like molecule, drives mesenchymal stem cell (MSC) to differentiate into osteoblast lineage through co-activation of Runx2-dependent gene transcription and repression of peroxisome proliferator-activated receptorγ (PPARγ)-dependent gene transcription. Dexamethasone (DEX), a synthetic and widely used glucocorticoid, affects osteogenesis. However, the signaling pathway by which DEX affects osteoblastic differentiation remains obscure. In this study, we found that DEX at the concentration of 10^{-8} M enhanced calcium deposition, TAZ, bone morphogenetic protein 2 (BMP-2) and alkaline phosphatase (ALP) expression during osteoblastic differentiation. RU486, an antagonist of glucocorticoid receptor, blocked the improvement of TAZ expression while MSCs were treated with 10^{-8} M DEX. Moreover, higher concentration (10^{-7} M) of DEX robustly suppressed TAZ and ALP expression in MSCs. These findings suggest that TAZ is not only involved in the signal pathway of BMP-2-induced osteoblastic differentiation, but also involved in the signaling pathway of DEX-induced osteoblastic differentiation, supporting the notion that TAZ is a convergence point of two signaling pathways, BMP-2 signaling pathway and Wnt-β-catenin signaling pathway.

1. Introduction

Mesenchymal stem cells (MSCs) constitute a small population of pluripotent cells within the bone marrow, which differentiate into adipocytes, chondrocytes, myocytes and osteoblasts under the influence of particular signaling [1]. TAZ (transcriptional coactivator with PDZ-binding motif), a β-catenin-like molecule, has been linked with the development of bone, fat, limb, kidney, muscle, heart and lung tissues [2–7], and functions as a molecular rheostat, promoting MSC differentiation into osteoblastic lineages by coactivating Runx2/Cbfa1 and blocking MSC differentiation into adipocyte lineages by repressing peroxisome proliferator-activated receptorγ (PPARγ)-dependent gene transcription [6–8]. Bone morphogenetic protein 2 (BMP-2) has been proven to induce bone formation both *in vivo* and *in vitro* [9]. In BMP-2-induced osteoblastic differentiation, TAZ level in MSCs is increased by several folds within a few days [7].

Dexamethasone (DEX), a synthetic glucocorticoid, can induce osteoporosis and even pathologic fracture when it is administrated at long-term and over-dose [10]. Since normal bone turnover depends on a balance between osteoblasts and osteoclasts, it is suggested that DEX may suppress osteoblast differentiation both *in vivo* and *in vitro*. DEX has been revealed to inhibit osteoblastic differentiation through the repression of BMP-2 expression, which in turn leads to a decrease in bone formation [11], and DEX redirect the differentiation of bone marrow stromal cells from the osteoblastic lineage to the adipocyte lineage [12]. However, most studies argue that DEX *in vitro* enhances the osteoblastic differentiation, alkaline phosphatase (ALP) activity and bone mineralization [13–17]. Thus, whether DEX inhibits or promotes osteoblastic differentiation and bone formation in MSCs remains controversial [18], and biological mechanism and signaling pathway by which DEX affects osteoblastic differentiation remain obscure.

In this study, we demonstrated that DEX combining with ascorbic acid (AA) and β-glycerophosphate (β-GP) *in vitro* not only robustly promoted bone formation, but also improved TAZ expression. DEX enhanced osteoblastic differentiation and increased TAZ expression in MSCs depending on its concentration in culture medium. These findings suggest that TAZ could be one of the key molecules in DEX-induced osteoblastic differentiation in rat MSCs.

* Corresponding author. Tel.: +86 576 85199876.
** Corresponding author. Tel.: +86 571 88208088.
E-mail addresses: hxchen-1@163.net (H.-X. Chen), Lijichen@zju.edu.cn (J.-C. Li).

0960-0760/$ – see front matter © 2009 Elsevier Ltd. All rights reserved.
doi:10.1016/j.jsbmb.2009.05.007

2. Materials and methods

2.1. Experimental animals and rat MSCs isolation

All animal experiments were approved by the Local Ethics Committee for Animal Care and Use of Zhejiang University in China. Sixteen 4-week-old virgin female Sprague–Dawley rats weighing approximately 150 g were purchased from Zhejiang University Animal Center (Hangzhou, China). Rats were euthanized by CO_2, and the bilateral femora and tibias were dissected under aseptic conditions. The bone marrow cells were flushed out of the femora and tibias with Dulbecco's modified Eagle's medium–low glucose (DMEM–LG, Gibco, NY, USA) by a 5-ml syringe. The marrow cells were seeded at a concentration of $5 \times 10^5/cm^2$ in 30 ml plastic flasks (Corning, USA) containing DMEM–LG supplemented with 10% fetal calf serum (Gibco, Milan, Italy), 1% glutamine (Sigma, St. Louis, MO), and 1% penicillin–streptomycin (Sigma). The cells were then incubated in 5% CO_2 at 37 °C, and the medium was changed every 3 days. When the cells reached 80% confluency in the flasks, cells were trypsinized (0.25% trypsin, GIBCO, Canada) and expanded into plates as passage 1.

2.2. Surface antigens of cultured cells

Surface antigens of cultured cells were detected as described previously [19]. The passage 1 MSCs were harvested and the cell density was adjusted to 1×10^7 cells/ml with PBS. Then the cells were labelled with CD34-FITC, CD90-PE, CD14-PerCP CD14-PerCP, and CD54-APC at 4 °C in the dark for more than 30 min, washed once with PBS and subjected to surface antigen assays by flow cytometry.

2.3. Induction of osteoblastic, adipogenic and chondrogenic differentiation in rat MSCs

Rat MSCs from passage 1 were seeded in 6-well plates at the concentration of $5 \times 10^5/cm^2$. After pre-cultured for 24 h, the MSCs were allowed to grow in different osteoblastic differentiation media according to the experimental requirements for up to 14 days. All MSCs were incubated in 5% CO_2 at 37 °C, and the medium was replaced every 3 days before harvest.

To induce adipogenic differentiation, rat MSCs were cultured for 14 days in DMEM–LG supplemented with 10^{-8} M DEX and 5 μg/ml insulin [20]. MSCs were fixed with 4% cold paraformaldehyde in PBS (pH 7.4) at room temperature for 15 min. Then the plates were washed three times with distilled water and incubated with Oil Red O (Sigma) solution for 5 min at room temperature.

To induce chondrogenic differentiation, aliquots of 2.5×10^5 MSCs were centrifuged at 1000 rpm for 5 min in 15 ml polypropylene conical tubes to form pellets, which were then cultured in high glucose DMEM supplemented with 1% ITS-Premix (Becton-Dickinson, USA), 50 mg/ml AA, 10^{-3} M sodium pyruvate, 10^{-7} M DEX, and 10 ng/ml of transforming growth factor-β3 (R&D Systems, Minneapolis, MN) for 28 days. Then the pellets were fixed with 4% paraformaldehyde, embedded in paraffin, and subjected to Safranin-O staining to confirm chondrogenic differentiation.

2.4. AR-S staining for mineralization

The mineralization of MSCs was performed in 6-well plates using Alizarin red staining (AR-S). Briefly, 6-well plates were washed twice with PBS (pH 7.4) and fixed with 4% cold paraformaldehyde in PBS (pH 7.4) at room temperature for 15 min. Then the plates were washed three times with distilled water and incubated with 40 mmol/l Alizarin Red-S (pH 4.2, Sigma) for 10 min at room temperature. The cells were then washed thoroughly with deionized water and observed using a converted microscope.

2.5. ALP activity assay

The MSCs were harvested and resuspended in 250 μl of culture supernatants, followed by cell breaking with an ultrasound breaker. After centrifugation, the ALP activities in the cell supernatants were quantified by an ALP Detection Kit (Nanjing Jiancheng Biotechnology Institute, Nanjing, China) and a spectrophotometer (Bio-Rad, Hercules, CA, USA) at a wavelength of 520 nm. Each value was normalized to the protein concentration.

2.6. RNA isolation

Total RNA was isolated by using TRIzol reagent (Invitrogen, Carlsbad, CA, USA) according to the manufacturer's protocol. RT-PCR was performed by M-MLV Reverse Transcriptase (Invitrogen, Carlsbad, CA) according to the manufacturer's specifications. Briefly, first-strand cDNAs were synthesized at 37 °C for 1 h in 20 μl reaction mixture using 2 μg isolated mRNA. The serially diluted first-strand cDNA samples were used as templates (DongSheng Inc., Beijing, China).

2.7. Reverse transcriptase PCR (RT-PCR) and real-time PCR

For RT-PCR, the diluted first-strand cDNA samples were amplified using a TaqDNA polymerase (DongSheng Inc., Beijing, China). The mRNA expression levels for TAZ, ALP, BMP-2, Runx2 and GAPDH were analyzed by Gel Image System 4.00 (Tannon Inc., Shanghai, China) and the relative expression of the mRNAs was normalized by dividing the ALP, BMP-2 or Runx2 values by the respective GAPDH values. For real-time PCR quantification, the RNA levels for the GRPDH were assayed in all samples as an internal control. Messenger RNA measurements were normalized using a robust global normalization algorithm. All control threshold cycle (Ct) values were corrected by the median difference in all samples from GRPDH. Messenger RNA levels were calculated relative to GRPDH mRNA. Real-time PCR was carried out in a 25-μl volume with SYBR Green PCR Master Mix (Applied Biosystems, Foster City, CA). Reactions were carried out and fluorescence was detected on an ABI 7700 system (PE Applied Biosystems). Primer sequences for the RT-PCR and real-time PCR were listed as follows: TAZ: 5′-AGGATCAGGATGCGTCAAG -3′ (forward) and 5′-CCAAAGTCCCGAGGTCAA-3′ (reverse); BMP-2: 5′-GGACTGCGGTCTCCTAAA-3′ and 5′-CAGCCTCAACTCAAACTCG-3′; GAPDH: 5′-GTTCAACGGCACAGTCAA-3′ and 5′-ATGAGCCCTTCCACGAT-3′; Runx2: 5′-GCCGGGAATGATGAGAACTA-3′ and 5′-GGACCGTCCACTGTCACTTT-3′; ALP: 5′-ACGGTGAACGGGAGAAC-3′ and 5′-CTCAGAACAGGGTGCGTAG-3′.

2.8. Western blot analysis

Fifty micrograms of total protein isolated from MSCs were mixed with sample buffer and heated at 80 °C for 10 min. Samples were subjected to 12% SDS-PAGE in 1× TGS (Tris–glycine SDS) at 100 mV for 1 h. Proteins were then transferred to PVDF membranes using a semi-dry transfer apparatus (Biorad) at 15 mV for 1 h at room temperature. Membranes were blocked using 1% BSA for 1 h at room temperature. Primary goat anti-TAZ antibody (1:1000, Santa Cruz Biotechnology, CA, USA) was added to blocking buffer overnight at 4 °C. The next day, membranes were washed five times in 1× TTBS (Tween®/Tris-buffered salt solution), 5 min each, on a shaker. The blot was then incubated with Cruz Marker™ compatible donkey anti-goat IgG-HRP (1:2000, Santa Cruz Biotechnology) for 1 h at room temperature. The blot was washed in TTBS for five times, 5 min each time. Proteins were visualized using ECL™ western blotting detection reagents (GE Healthcare, Buckinghomshire, UK) and signals

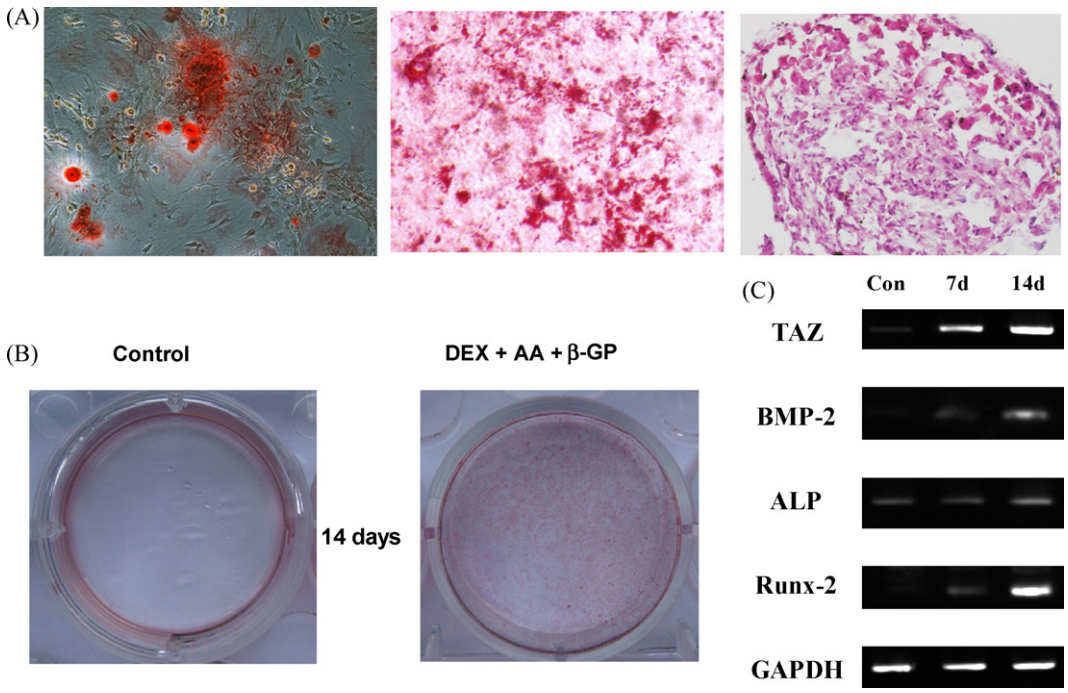

Fig. 1. (A) Multilineage differentiation of rat MSCs. Left: osteoblast differentiation (AR-S, 100×); middle: adipogenic differentiation (Oil Red O staining, 100×); right chondrogenic differentiaion (Safranin-O staining, 40×). (B) MSCs were cultured without (control) or with 10^{-8} M DEX combined with 10^{-2} M β-GP and 50 μg/ml AA and stained for calcium deposition using Alizarin Red-S at 14 days. (C) Enhanced mRNA expression of TAZ, BMP-2, ALP, and Runx2 by RT-PCR after MSCs cultured without (Con) or with 10^{-8} M DEX combined with 10^{-2} M β-GP and 50 μg/ml AA for 7 and 14 days.

were detected using Image Station 4000R (Kodak, New Haven, CT, USA).

2.9. Immunocytochemistry

MSCs were fixed with 4% paraformaldehyde in PBS (pH 7.4), permeabilized with 0.5% Triton X-100 in PBS, and washed with PBS at room temperature. After blocking with 5% milk in PBS, cells were incubated with the goat anti-TAZ antibody (1:200, Santa Cruz Biotechnology, CA, USA) at 4 °C for 12 h. Cells were proceeded to incubate with Cruz Marker™ compatible donkey anti-goat IgG-HRP (1:500, Santa Cruz Biotechnology, CA, USA) at 37 °C for 1 h. Washed again with PBS for three times, then, the staining was developed with a DAB Staining kit according to the manufac-

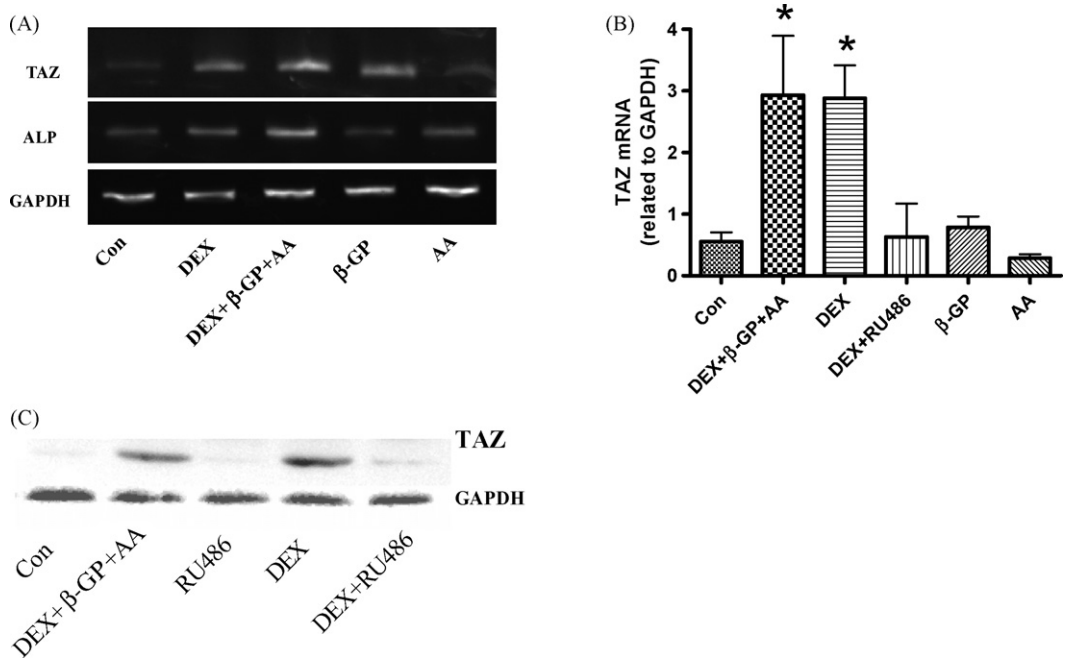

Fig. 2. Rat MSCs were cultured in different media for 7 days by (A) RT-PCR. Lanes—1: control; 2: 10^{-8} M DEX; 3: 10^{-8} M DEX + 50 μg/ml AA + 10^{-2} M β-GP; 4: 10^{-2} M β-GP; 5: 50 μg/ml AA; (B) TAZ mRNA expression by real-time PCR. Lanes—1: control; 2: 10^{-8} M DEX + 50 μg/ml AA + 10^{-2} M β-GP; 3: 10^{-8} M DEX; 4: 10^{-8} M DEX + 10^{-5} M RU486; 5: 10^{-2} M β-GP; 6: 50 μg/ml AA; (C) Western blot. Lanes—1: control; 2: 10^{-8} M DEX + 50 μg/ml AA + 10^{-2} M β-GP; 3: 10^{-5} M RU486; 4: 10^{-8} M DEX; 5: 10^{-8} M DEX + 10^{-5} M RU486. $^{*}P < 0.05$.

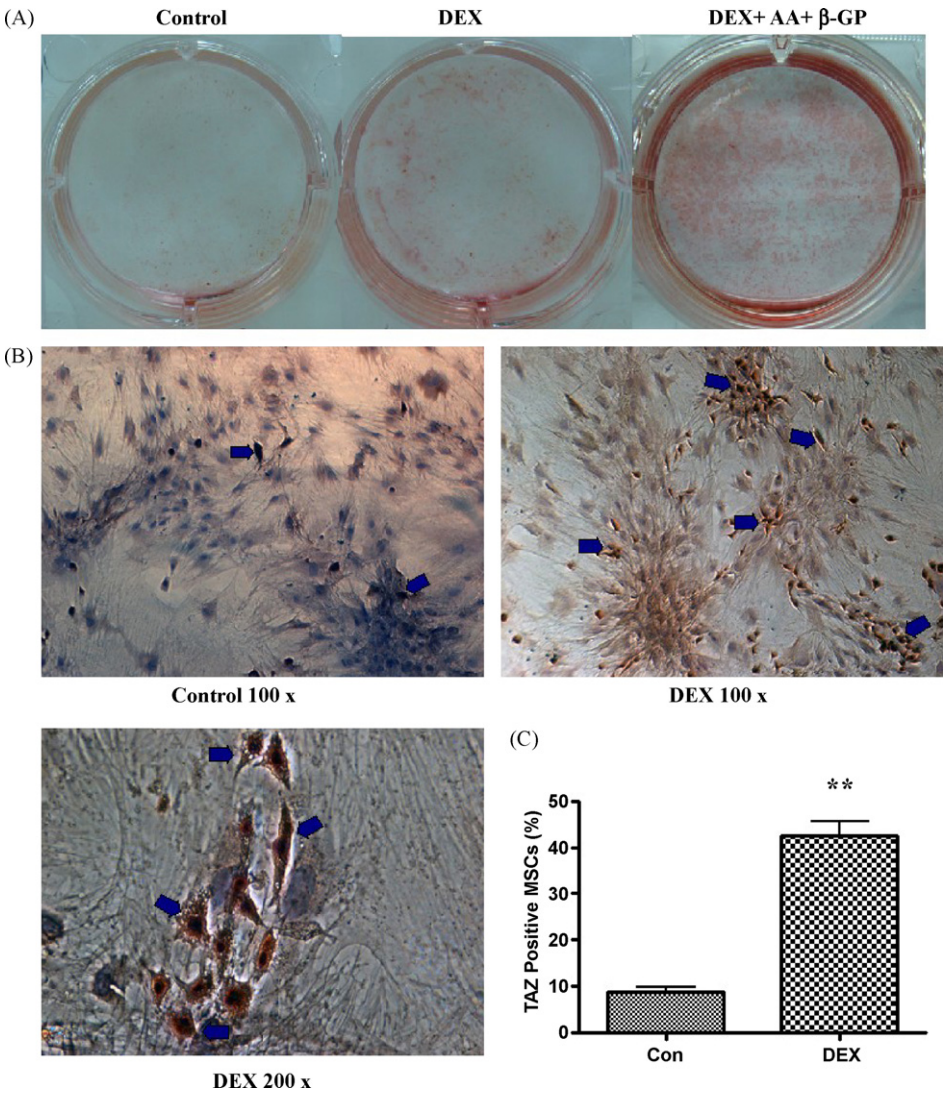

Fig. 3. 10^{-8} M DEX enhanced calcium deposition and TAZ expression in cultured rat MSCs. (A) Cells were cultured in the absence (left) and presence of 10^{-8} M DEX (middle), and 10^{-8} M DEX together with 50 μg/ml AA, and 10^{-2} M β-GP (right) for 14 days. Cultures were stained for calcium deposition using Alizarin Red-S. (B) Immunocytochemistry demonstrated TAZ-positive cells (blue arrows). Upper left: control, 100×; upper right: MSCs were treated with 10^{-8} M DEX for 14 days, 100×. Lower left: the TAZ-positive cells using immunocytochemistry were in the shape of spindle, polygon, and cube (blue arrows, 200×). (C) Comparison of percentage of TAZ-positive MSCs. $^{**}P < 0.01$. (For interpretation of the references to color in this figure legend, the reader is referred to the web version of the article.)

turer's protocol (ZSGB-BIO, Beijing, China) and visualized by using a converted microscope. The TAZ-positive MSCs were analyzed by imagine software, NIS-Element D 2.20 (Nikon, Kanagawa, Japan).

2.10. Statistical analysis

Data were expressed as mean ± SEM. Differences among groups were analyzed by one-way ANOVA. In the case of two groups, a Student's *t*-test was used. Statistical significance was assessed at $P < 0.05$. Experiments were independently triplicated and results were qualitatively identical. Representative experiments are shown.

3. Results

3.1. Surface antigen identification and multilineage differentiation of MSCs

The isolated cells were identified by flow cytometry for assaying CD34-FITC, CD90-PE, CD14-PerCP CD14-PerCP, and CD54-APC as previously described [19]. In the present study, the results revealed that isolated cells were $CD54^+$ and $CD90^+$ but $CD14^-$ and $CD34^-$. After cultured in osteoblast differentiation medium (10^{-8} M DEX, 10^{-2} M β-GP and 50 μg/ml AA) for 14 days, AR-S revealed calcium deposit nodules in MSCs (Fig. 1A, left). In adipogenic differentiation, the MSCs were cultured in adipogenic medium for 14 days, Oil Red O staining demonstrated positive staining in MSCs (Fig. 1A, middle). In chondrogenic differentiation, MSCs were induced in chondrogenic medium for 4 weeks, the MSCs were positive for Safranin-O stain and demonstrated chondrocyte morphology (Fig. 1A, right). The surface antigen identification and mutilineage differentiation ability supported that these isolated cells were MSCs.

3.2. TAZ expression in MSCs during osteoblastic differentiation

AR-S was performed to determine the mineralization in rat MSCs treated with 10^{-8} M DEX combined with 10^{-2} M β-GP and 50 μg/ml AA for 14 days. Treatment with DEX combined with β-GP and AA for 14 days robustly enhanced MSCs mineralization compared to vehicle control (Fig. 1B). To determine whether DEX combined with AA and β-GP increases the expression levels of osteoblastic factors dur-

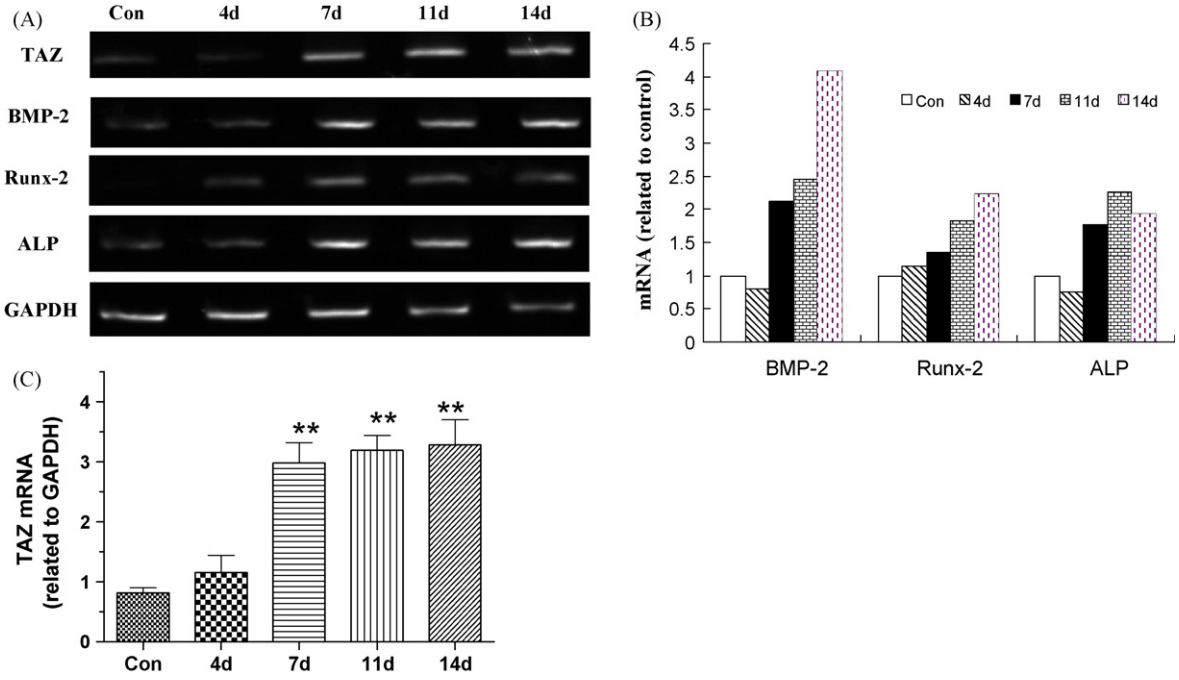

Fig. 4. 10^{-8} M DEX affects mRNA levels of TAZ, BMP-2, Runx2 and ALP in rat MSCs in 14 days. (A) RT-PCR for TAZ, BMP-2, Runx2, and ALP mRNA. (B) Semiquantitative analysis of BMP-2, Runx2 and ALP mRNA. (C) Analysis of TAZ mRNA level by real-time PCR. $^{*}P < 0.01$.

ing osteoblastic differentiation of MSCs, we further analyzed mRNA expression levels of TAZ, BMP-2, Runx2, and ALP (an osteoblastic differentiation marker) in MSCs by RT-PCR at days 0 (control), 7 and 14. Consistent with the ALP mRNA expression patterning which exhibited time-dependent increases during osteoblastic differentiation in MSCs (Fig. 1C), TAZ, BMP-2 and Runx2 mRNA expression levels at days 0, 7 and 14 showed time-dependent increases in rat MSCs after treatment with DEX combined with β-GP and AA (Fig. 1C).

To determine the osteoblastic differentiation under different treatment conditions, we further analyzed the TAZ and ALP mRNA levels in the first passage of rat MSCs growing in different differentiation media for 7 days. RT-PCR and real-time PCR demonstrated that 10^{-8} M DEX, 10^{-8} M DEX combined with AA and β-GP increased the TAZ mRNA expression in MSCs compared with control (Fig. 2A and B). MSCs treated with AA or β-GP did not increase TAZ expression compared with control (Fig. 2B). However, while MSCs were cultured with 10^{-8} M DEX combined with 10^{-5} M RU486, an antag-

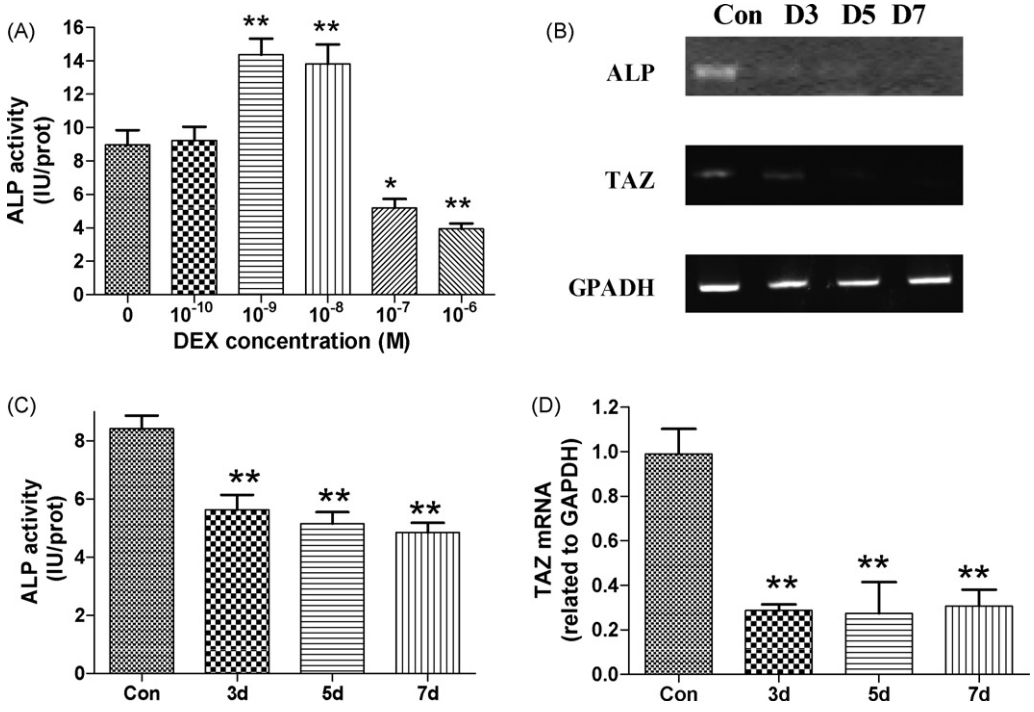

Fig. 5. (A) DEX dose-dependently affects ALP activity in rat MSCs at day 7; (B) 10^{-7} M DEX decreases mRNA of TAZ and ALP expression in rat MSCs by RT-PCR; (C) 10^{-7} M DEX inhibits ALP activity in rat MSCs at days 3, 5, and 7; (D) Analysis of TAZ mRNA level by real-time PCR. $^{*}P < 0.05$; $^{**}P < 0.01$.

onist of glucocorticoid receptor, TAZ mRNA level did not raise at day 7 compared with control (Fig. 2B). Immunobloting analysis also confirmed that TAZ protein levels increased at day 7 in MSCs treated with 10^{-8} M DEX or 10^{-8} M DEX combined with AA and β-GP, but not in MSCs treated with 10^{-5} M RU486 or 10^{-8} M DEX combined with 10^{-5} M RU486 (Fig. 2C).

3.3. Effect of 10^{-8} M DEX on calcium deposition and the number of TAZ-positive cells

To identify the ability of DEX in modulating osteoblastic differentiation of MSCs, rat MSCs were allowed to grow in three different media for 14 days: (1) DMEM–LG; (2) DMEM–LG containing 10^{-8} M DEX and (3) DMEM–LG containing 10^{-8} M DEX, 50 μg/ml AA and 10^{-2} M β-GP. AR-S staining revealed that DEX increased calcium deposition and the addition of AA and β-GP synergically increased calcium deposit ability of DEX (Fig. 3A). To further examine the osteoblastic effect of DEX, we immunohistochemically stained TAZ protein in MSCs treated with 10^{-8} M DEX for 14 days. The TAZ-positive cells exhibited in the shape of spindle, polygon, and cube (Fig. 3B). The number of TAZ-positive cells after DEX treatment significantly increased compared to control ($P < 0.01$) (Fig. 3C).

3.4. Effect of 10^{-8} M DEX on TAZ, BMP-2, Runx2 and ALP mRNA expression

The differentiation of MSCs into osteoblasts is critically dependent on Runx2 [21], and TAZ may function as an endogenous coactivator of Runx2 in cells [6]. We investigated the effects of DEX at 10^{-8} M on TAZ, BMP-2, Runx2 and ALP mRNA expression levels. 10^{-8} M DEX increased BMP-2, Runx2 and ALP mRNA levels by 2.1- and 4.0-fold, 1.5- and 2.1-fold, 1.8- and 1.9-fold at days 7 and 14, respectively by semiquantitative RT-PCR (Fig. 4A and B). In addition, at days 7, 11 and 14, 10^{-8} M DEX significantly increased TAZ mRNA expression by real-time PCR ($P < 0.01$) (Fig. 4A and C).

3.5. DEX at 10^{-7} M suppresses TAZ and ALP expression in MSCs

Previous studies suggested that DEX at higher concentration may inhibit osteoblastic differentiation [22–24]. We analyzed ALP activity in rat MSCs that were treated with different concentrations of DEX for 7 days. DEX at 10^{-8} M and 10^{-9} M significantly elevated ALP activity ($P < 0.01$) whereas 10^{-7} M DEX ($P < 0.05$) and 10^{-6} M DEX ($P < 0.01$) inhibited ALP activity in rat MSCs compared with control (Fig. 5A). Therefore we tested the effects of DEX at higher concentration (10^{-7} M) on TAZ and ALP expression levels as well as ALP activity. This concentration of DEX also significantly inhibited ALP mRNA levels and its activity (Fig. 5B and C). In contrast to the induction of TAZ expression by 10^{-8} M DEX, 10^{-7} M DEX significantly decreased the TAZ mRNA level by real-time PCR at days 3, 5 and 7 ($P < 0.01$) (Fig. 5B and D).

4. Discussion

In the present study, we demonstrated that during osteoblastic differentiation induced by 10^{-8} M DEX combined with β-GP and AA improved TAZ, Runx2, BMP-2 and ALP mRNA levels in rat MSCs. Lower concentration of DEX (10^{-8} M) promoted calcium formation, increased mRNA and protein level of TAZ in MSCs, while higher concentration of DEX (10^{-7} M) exerts the inhibitory effects.

It has been proven that BMP-2 increases TAZ level in MSCs by several folds during osteoblastic differentiation [7]. Present study showed that TAZ level in MSCs increased at days 7 and 14 while these cells were treated with 10^{-8} M DEX combined with 10^{-2} M β-GP and 50 μg/ml AA. The osteoblast differentiation maker ALP also showed time-dependent increases in rat MSCs during osteoblast differentiation. It is well known that Runx2, also called Cbfa1, controls the expression of osteoblast-specific genes (e.g., osteocalcin). TAZ has been proven to be a Runx2 transcription coactivator, which binds to Runx2 in the nucleus to regulate osteoblastic differentiation [24]. In this study, mRNA levels of BMP-2 and Runx2 also increased during the osteoblast differentiation (Fig. 1B).

So far, whether DEX inhibits or promotes osteoblastic differentiation and bone formation in MSCs remains controversial [18], and the signaling pathway by which DEX affects osteoblastic differentiation remain obscure. Present study showed that 10^{-8} M DEX increased calcium formation in MSCs at day 14 and the effect was synergized by AA and β-GP (Fig. 3A). Real-time PCR and immunobloting analysis showed that TAZ mRNA level and protein expression were enhanced in MSCs treated with 10^{-8} M DEX at day 7 (Fig. 2B and C). In addition, the number of TAZ-positive MSCs after 10^{-8} M DEX treatment significantly increased compared to control using immunochemistry assay (Fig. 3C). The stimulative effect of 10^{-8} M DEX on TAZ were blocked by 10^{-5} M RU486, an antagonist of glucocorticoid receptor (Fig. 2B and C) and MSCs were treated with AA or β-GP did not show increased TAZ level (Fig. 2B). In the present study,

DEX at 10^{-8} M and 10^{-9} M significantly elevated ALP activity ($P < 0.01$) whereas 10^{-7} M DEX ($P < 0.05$) and 10^{-6} M DEX ($P < 0.01$) inhibited ALP activity in rat MSCs (Fig. 5A). We also demonstrated that higher concentration of DEX (10^{-7} M) decreased TAZ mRNA level and ALP activity from days 3 to 7 (Fig. 5B–D), which indicates that TAZ level is closely related with osteoblast differentiation ability. Other authors also provided evidence that DEX has a dual role in osteoblastic differentiation depending on the applied concentration [14,17,22]. Therefore DEX at 10^{-8} M and 10^{-9} M may be the physiological concentration that is necessary for osteoblast differentiation in MSCs while DEX at higher concentration (10^{-7} M or higher than 10^{-7} M) may pharmacological, inhibiting osteoblast differentiation in MSCs and leading to glucocorticoid-induced osteoporosis.

Besides BMP-2 signaling, the Wnt-β-Catenin signaling pathway is likely to play an important role in regulating osteoblastic differentiation and skeletal development [25–28]. The β-catenin is an intracellular molecule node of the canonical Wnt signaling pathway [29], while TAZ is called a β-catenin-like molecule. The cytoplasmic β-catenin, via canonical Wnt signaling enter into the nucleus and heterodimerize with Lef/Tcf transcription factors to regulate Wnt target genes [29], enhancing expression of Runx2 and osteoblastic differentiation [30,31], repressing adipocyte differentiation [32,33]. Previous study indicated that DEX inhibits osteoblast differentiation by opposing Wnt-β-catenin signaling [12,24,34]. In this study, 10^{-7}M DEX may suppress osteoblastic differentiation in MSCs by opposing Wnt-β-catenin signaling, which lead to the decreased expression of TAZ. Therefore TAZ could be a key molecule in DEX-induced osteogenic differentiation.

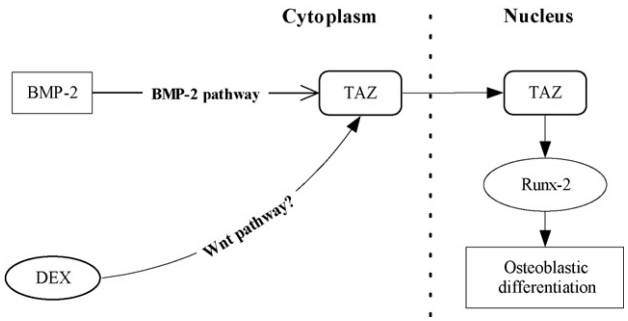

Fig. 6. Presumed role of TAZ convergence point of BMP-2 and Wnt signal pathway during osteoblastogenic differentiation.

In conclusion, this study revealed that DEX can affect TAZ expression during osteogenic differentiation in MSCs, which may depend on its concentration. These results suggest that TAZ is not only involved in the signaling pathway of BMP-2-induced osteogenic differentiation, but also in the signaling pathway of DEX-induced osteoblast differentiation. Therefore TAZ, a β-catenin-like molecule, may be convergence point of two signal pathways, BMP-2 signal pathway and Wnt-β-catenin signal pathway (Fig. 6).

Acknowledgements

This work is supported by the National Foundation for Fostering Talents of Basic Science (NFFTBS) (No. J0730856), Grant from the Science and Technology Department of Zhejiang Province (No. 2007C33025), and Scientific Research Fund of Taizhou Hospital of Wenzhou Medical College. We thank Dr. Ouyang Hongwei, Dr. Song Xinhui, Dr. Wu Ximei, and Dr. Wang Qingqing, School of Medicine, Zhejiang University, for their technical assistance in isolation, culture, and multilineage differentiation identification of MSCs.

References

[1] M.F. Pittenger, A.M. Mackay, S.C. Beck, R.K. Jaiswal, R. Douglas, J.D. Mosca, M.A. Moorman, D.W. Simonetti, S. Craig, D.R. Marshak, Multilineage potential of adult human mesenchymal stem cells, Science 284 (1999) 143–147.
[2] R. Makita, Y. Uchijima, K. Nishiyama, T. Amano, Q. Chen, T. Takeuchi, A. Mitani, T. Nagase, Y. Yatomi, H. Aburatani, O. Nakagawa, E.V. Small, P. Cobo-Stark, P. Igarashi, M. Murakami, J. Tominaga, T. Sato, T. Asano, Y. Kurihara, H. Kurihara, Multiple renal cysts, urinary concentration defects, and pulmonary emphysematous changes in mice lacking TAZ, Am. J. Physiol. Renal Physiol. 294 (2008) F542–F553.
[3] Y. Tian, R. Kolb, J.H. Hong, J. Carroll, D. Li, J. You, R. Bronson, M.B. Yaffe, J. Zhou, T. Benjamin, TAZ promotes PC2 degradation through a SCFbeta-Trcp E3 ligase complex, Mol. Cell. Biol. 27 (2007) 6383–6395.
[4] M. Murakami, M. Nakagawa, E.N. Olson, O. Nakagawa, A WW domain protein TAZ is a critical coactivator for TBX5, a transcription factor implicated in Holt-Oram syndrome, Proc. Natl. Acad. Sci. U.S.A. 102 (2005) 18034–18039.
[5] W.M. Mahoney Jr., J.H. Hong, M.B. Yaffe, I.K. Farrance, The transcriptional co-activator TAZ interacts differentially with transcriptional enhancer factor-1 (TEF-1) family members, Biochem. J. 388 (2005) 217–225.
[6] J.H. Hong, E.S. Hwang, M.T. McManus, A. Amsterdam, Y. Tian, R. Kalmukova, E. Mueller, T. Benjamin, B.M. Spiegelman, P.A. Sharp, N. Hopkins, M.B. Yaffe, TAZ, a transcriptional modulator of mesenchymal stem cell differentiation, Science 309 (2005) 1074–1078.
[7] J.H. Hong, M.B. Yaffe, TAZ: a beta-catenin-like molecule that regulates mesenchymal stem cell differentiation, Cell Cycle 5 (2006) 176–179.
[8] F. Kanai, P.A. Marignani, D. Sarbassova, R. Yagi, R.A. Hall, M. Donowitz, A. Hisaminato, T. Fujiwara, Y. Ito, L.C. Cantley, M.B. Yaffe, TAZ: a novel transcriptional co-activator regulated by interactions with 14-3-3 and PDZ domain proteins, EMBO J. 19 (2000) 6778–6791.
[9] P. De Biase, R. Capanna, Clinical applications of BMPs, Injury 36 (Suppl. 3) (2005) S43–S46.
[10] A.D. Woolf, An update on glucocorticoid-induced osteoporosis, Curr. Opin. Rheumatol. 19 (2007) 370–375.
[11] C.A. Luppen, E. Smith, L. Spevak, A.L. Boskey, B. Frenkel, Bone morphogenetic protein-2 restores mineralization in glucocorticoid-inhibited MC3T3-E1 osteoblast cultures, J. Bone Miner. Res. 18 (2003) 1186–1197.
[12] E. Canalis, Mechanisms of glucocorticoid action in bone, Curr. Osteoporos. Rep. 3 (2005) 98–102.
[13] N.R. Jorgensen, Z. Henriksen, O.H. Sorensen, R. Civitelli, Dexamethasone, BMP-2, and 1,25-dihydroxyvitamin D enhance a more differentiated osteoblast phenotype: validation of an in vitro model for human bone marrow-derived primary osteoblasts, Steroids 69 (2004) 219–226.
[14] M. Eijken, M. Koedam, M. van Driel, C.J. Buurman, H.A. Pols, J.P. van Leeuwen, The essential role of glucocorticoids for proper human osteoblast differentiation and matrix mineralization, Mol. Cell. Endocrinol. 248 (2006) 87–93.
[15] Y. Liu, A. Porta, X. Peng, K. Gengaro, E.B. Cunningham, H. Li, L.A. Dominguez, T. Bellido, S. Christakos, Prevention of glucocorticoid-induced apoptosis in osteocytes and osteoblasts by calbindin-D28k, J. Bone Miner. Res. 19 (2004) 479–490.
[16] T.L. Chen, Inhibition of growth and differentiation of osteoprogenitors in mouse bone marrow stromal cell cultures by increased donor age and glucocorticoid treatment, Bone 35 (2004) 83–95.
[17] H. Atmani, D. Chappard, M.F. Basle, Proliferation and differentiation of osteoblasts and adipocytes in rat bone marrow stromal cell cultures: effects of dexamethasone and calcitriol, J. Cell. Biochem. 89 (2003) 364–372.
[18] D. Hong, H.X. Chen, R.S. Ge, J.C. Li, The biological roles of extracellular and intracytoplasmic glucocorticoids in skeletal cells, J. Steroid Biochem. Mol. Biol. 111 (2008) 164–170.
[19] X.C. Wan, C.P. Liu, M. Li, D. Hong, D.M. Li, H.X. Chen, J.C. Li, Staphylococcal enterotoxin C injection in combination with ascorbic acid promotes the differentiation of bone marrow-derived mesenchymal stem cells into osteoblasts in vitro, Biochem. Biophys. Res. Commun. 373 (2008) 488–492.
[20] S. Meirelles Lda, N.B. Nardi, Murine marrow-derived mesenchymal stem cell: isolation, in vitro expansion, and characterization, Br. J. Haematol. 123 (2003) 702–711.
[21] T. Komori, H. Yagi, S. Nomura, A. Yamaguchi, K. Sasaki, K. Deguchi, Y. Shimizu, R.T. Bronson, Y.H. Gao, M. Inada, M. Sato, R. Okamoto, Y. Kitamura, S. Yoshiki, T. Kishimoto, Targeted disruption of Cbfa1 results in a complete lack of bone formation owing to maturational arrest of osteoblasts, Cell 89 (1997) 755–764.
[22] N. Leclerc, C.A. Luppen, V.V. Ho, S. Nagpal, J.G. Hacia, E. Smith, B. Frenkel, Gene expression profiling of glucocorticoid-inhibited osteoblasts, J. Mol. Endocrinol. 33 (2004) 175–193.
[23] Y. Engelbrecht, H. de Wet, K. Horsch, C.R. Langeveldt, F.S. Hough, P.A. Hulley, Glucocorticoids induce rapid up-regulation of mitogen-activated protein kinase phosphatase-1 and dephosphorylation of extracellular signal-regulated kinase and impair proliferation in human and mouse osteoblast cell lines, Endocrinology 144 (2003) 412–422.
[24] E. Smith, B. Frenkel, Glucocorticoids inhibit the transcriptional activity of LEF/TCF in differentiating osteoblasts in a glycogen synthase kinase-3beta-dependent and -independent manner, J. Biol. Chem. 280 (2005) 2388–2394.
[25] D.A. Glass 2nd, G. Karsenty, Canonical Wnt signaling in osteoblasts is required for osteoclast differentiation, Ann. N.Y. Acad. Sci. 1068 (2006) 117–130.
[26] H. Hu, M.J. Hilton, X. Tu, K. Yu, D.M. Ornitz, F. Long, Sequential roles of Hedgehog and Wnt signaling in osteoblast development, Development 132 (2005) 49–60.
[27] M.P. Yavropoulou, J.G. Yovos, The role of the Wnt signaling pathway in osteoblast commitment and differentiation, Hormones (Athens) 6 (2007) 279–294.
[28] D.A. Glass 2nd, G. Karsenty, In vivo analysis of Wnt signaling in bone, Endocrinology 148 (2007) 2630–2634.
[29] D.A. Glass 2nd, G. Karsenty, Molecular bases of the regulation of bone remodeling by the canonical Wnt signaling pathway, Curr. Top. Dev. Biol. 73 (2006) 43–84.
[30] T. Gaur, C.J. Lengner, H. Hovhannisyan, R.A. Bhat, P.V. Bodine, B.S. Komm, A. Javed, A.J. van Wijnen, J.L. Stein, G.S. Stein, J.B. Lian, Canonical WNT signaling promotes osteogenesis by directly stimulating Runx2 gene expression, J. Biol. Chem. 280 (2005) 33132–33140.
[31] G. Mbalaviele, S. Sheikh, J.P. Stains, V.S. Salazar, S.L. Cheng, D. Chen, R. Civitelli, Beta-catenin and BMP-2 synergize to promote osteoblast differentiation and new bone formation, J. Cell. Biochem. 94 (2005) 403–418.
[32] S.E. Ross, N. Hemati, K.A. Longo, C.N. Bennett, P.C. Lucas, R.L. Erickson, O.A. MacDougald, Inhibition of adipogenesis by Wnt signaling, Science 289 (2000) 950–953.
[33] J. Liu, S.R. Farmer, Regulating the balance between peroxisome proliferator-activated receptor gamma and beta-catenin signaling during adipogenesis. A glycogen synthase kinase 3beta phosphorylation-defective mutant of beta-catenin inhibits expression of a subset of adipogenic genes, J. Biol. Chem. 279 (2004) 45020–45027.
[34] K. Ohnaka, M. Tanabe, H. Kawate, H. Nawata, R. Takayanagi, Glucocorticoid suppresses the canonical Wnt signal in cultured human osteoblasts, Biochem. Biophys. Res. Commun. 329 (2005) 177–181.